Modified Spline-based Path Planning for Autonomous Ground Vehicle

Evgeni Magid[1], Roman Lavrenov[1] and Airat Khasianov[2]
[1]*Intelligent Robotics Department, Higher School of Information Technology and Information Systems, Kazan Federal University, Kremlyovskaya str. 35, Kazan, Russian Federation*
[2]*Higher School of Information Technology and Information Systems, Kazan Federal University, Kremlyovskaya str. 35, Kazan, Russian Federation*

Keywords: Path Planning, Voronoi Diagram, Potential Field, Mobile Robot.

Abstract: Potential function based methods play significant role in global and local path planning. While these methods are characterized with good reactive behavior and implementation simplicity, they suffer from a well-known problem of getting stuck in local minima of a navigation function. In this article we propose a modification of our original spline-based path planning algorithm for a mobile robot navigation, which succeeds to solve local minima problem and adds additional criteria of start and target points visibility to help optimizing the path selection. We apply a Voronoi graph based path as an input for iterative multi criteria optimization algorithm. The algorithm was implemented in Matlab environment and simulation results demonstrate that we succeeded to overcome our original algorithm pitfalls.

1 INTRODUCTION

Today most robotic applications are targeting for industrial production speed and quality improvement as well as for human replacement in various scenarios, which range from social-oriented human-robot interaction scenarios (Pipe et al., 2014) to dangerous for a human urban search and rescue scenarios (Magid et al., 2011). The later scenarios may include indoor and outdoor environments and require good performance in autonomous navigation within unknown environments (Indelman et al., 2015), ability to deal with computational complexity of simultaneous localization and mapping (SLAM) (Buyval et al., 2016), capabilities of negotiation and collaboration (Panov and Yakovlev, 2017) with other robots within a team (Rosenfeld et al., 2015) or swarm control (Ronzhin et al., 2016) and other functionality.

Path planning is probably the most essential part of autonomous navigation for a mobile robot, which is responsible for providing a collision-free path between initial and goal positions of the robot. A good path planning algorithm should guarantee its completeness, i.e. the robot should reach its goal position or conclude explicitly that a path, which could connect the start and the goal positions, does not exist. The completeness property is by default incorporated into all global path planning methods, but for local path planning in order to satisfy this property various strategies are applied. The classical global path planning approach, which is referred as *piano movers problem*, utilizes complete *a priori* knowledge about environment: a robot is aware of its own shape, initial and goal position and orientation, and a set of 2D or 3D environment obstacles, where each obstacle information includes precisely defined shape, position, orientation in space and other task-related data (e.g., texture or traversability index (Seraji, 1999)). Next, the robot searches for a continuous path from the initial position to the goal position, while negotiating with static obstacles of the environment along its way. In order to simplify the procedures, often the concept of multi-dimensional configuration space (Latombe, 2012) is applied for the planning. In such settings, the path planning operation becomes an off-line onetime operation since a complete knowledge about the environment is available in advance. This allows optimizing a solution with regard to various criteria in order to obtain an optimal or at least sub-optimal path relatively to these criteria. The path search algorithm should consider such qualities as ability to generate a collision free path, time and space complexity, ability to discover a path if it does exist, efficient computational scheme, and the later is actually the main difficulty of the piano movers approach. Yet, in real world scenario the robot does not possess a complete knowledge about environment - except some very limited or artificial application cases. For this reason the robot

Magid, E., Lavrenov, R. and Khasianov, A.
Modified Spline-based Path Planning for Autonomous Ground Vehicle.
DOI: 10.5220/0006442601320141
In *Proceedings of the 14th International Conference on Informatics in Control, Automation and Robotics (ICINCO 2017) - Volume 2*, pages 132-141
ISBN: Not Available

should continuously collects sensory data from its potentially dynamic environment and plan the path accordingly, which requires a reasonable combination of local and global methods of path planning.

When a robot uses incoming sensory data to create a global world map as it traverses the environment, we refer to such approach as global sensor-based planning. Next, the created map is used for path planning. Main weakness of global sensor-based planning approach is a significant computational burden on the robot while creating and maintaining a global model as well as excessive memory requirements in order to store the model and the large amount of sensory information, which is associated with the model. Purely local path-planners avoid these issues by utilizing only local sensory information; this allows to reactively negotiate environmental obstacles but does not guarantee global convergence. This way, in order to provide a superior performance, a well-balanced integration of global and local path-planners is essential.

A classical and popular path planning approach applies potential field method (Tang et al., 2010), (Khatib and Siciliano, 2016), which is based on an artificial potential field concept that marks a goal position as an attractive pole and obstacles are represented with repulsive surfaces. Then a robot pursues the potential gradient in the direction of its minimum. Potentials are generated either at a global or a local level and this is a matter of available environmental information (Andrews and Hogan, 1983). Potential field methods gained their popularity due to algorithm simplicity and a capability of fast reactive avoidance of mobile and stationary obstacles. However, potential field methods are typically featured with such drawbacks as path oscillations for certain configurations of obstacles (e.g., narrow passages) and local minima problem, which captures a robot in a potential function local valley and requires special escape procedure in order to proceed (e.g., sequence of random steps in arbitrary direction).

In our previous research we had proposed a path planning spline-based algorithm for a car-like mobile robot within a well-known environment (Magid et al., 2006). It uses potential field method for obstacle collision avoidance to provide a locally sub-optimal path with regard to path length, path smoothness and safety optimization criteria. While a typical path-planning algorithm applies final smoothing of a path at the last stages only (Fleury et al., 1995), (Elbanhawi et al., 2015), our algorithm special feature is the smoothness criterion integration into path optimization from the first stage of the algorithm. Other criteria (path length and safety) played secondary role in optimization procedure and thus collision-free but not sufficiently smooth path was treated as a low quality one. In order to improve the original algorithm performance, to add flexibility for path optimization and a possibility for a fast dynamic replanning in a case the initially off-line selected path becomes unavailable, we integrate Voronoi Diagram approach into our algorithm (Choset and Burdick, 1995).

The rest of the paper is organized as follows. Section 2 briefly describes our previous research within spline-based path planning. In section 3 we present new criteria that improve the algorithm performance and add more flexibility for the user while selecting path evaluation measures. Section 4 presents our modification of the spline-based algorithm, which successfully overcomes the weaknesses of the initial approach. Section 5 demonstrates the original and the new algorithm trial examples, where the new algorithm shows successful solution of the original algorithm failures. Section 6 discusses our future work. Finally, we conclude in Section 7.

2 SPLINE-BASED ROBOT NAVIGATION WITH ORIGINAL POTENTIAL FIELD APPROACH

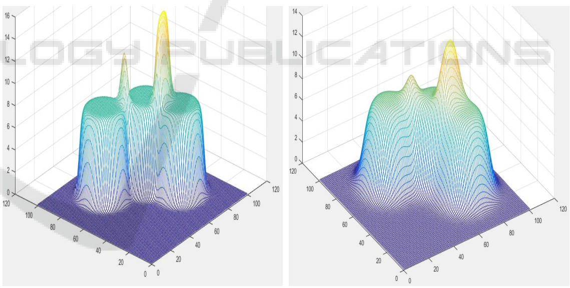

Figure 1: Repulsive potential function of eq. 1 for $\alpha = 0.5$ (left) and $\alpha = 0.2$ (right) that corresponds to the obstacles in Figure 4.

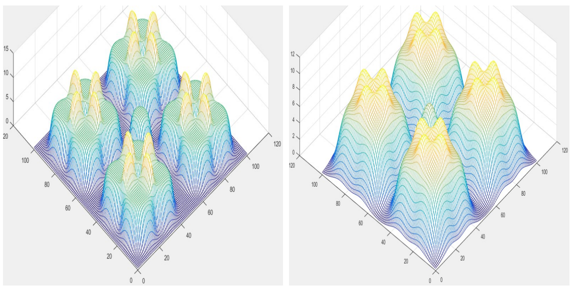

Figure 2: Repulsive potential function of eq. 1 for $\alpha = 0.5$ (left) and $\alpha = 0.2$ (right) that corresponds to the obstacles in Figure 5.

The spline-based method, proposed by Magid et.al. about a decade ago (Magid et al., 2006) navigates a car-like robot in a planar known environment populated with static obstacles. The algorithm is considering an omnidirectional circle-shape robot which reduces a search space by one dimension (an orientation) and all further actions are performed for a point robot in a 2D configuration space. An obstacle is presented with a set of intersecting circles of different sizes and each set may contain just a single circle or a finite number of circles. The idea behind such restriction is based on the assertion that any arbitrary obstacle could be well-approximated with a finite set of circles. Next, given a complete information about the environment, a start and a target positions of the robot, the robot searches for a collision-free path which is guided by a pre-determined cost function. The details of the algorithm could be found in (Magid et al., 2006), while in this section we briefly describe the selected cost functions and overview the algorithm, and demonstrate a successful example of its execution and two failing examples. Finally, we explain the origins of these failures in subsection 2.3 and further suggest its modification in Section 4.

2.1 Cost Function

To provide the collision free path, a repulsive potential function is featured with a high value inside an obstacle and on its border and a small value within free space. This way, high value of the potential function in the obstacle's centre pushes all points of a path outside in order to minimize path cost during local optimization procedure. The potential field begins to drastically change (decline) on obstacle's border, keeps decreasing with distance as a point moves away from the border and becomes zero rather fast in a close vicinity of the obstacle. Assuming the robot's position at $q(t) = (x(t), y(t))$ for a time-stamp t, a contribution of a single circle (where the circle is a part of an obstacle) repulsive potential to the global potential function is defined with the following equation:

$$U_{rep}(q) = 1 + \tanh(\alpha(\rho - \sqrt{(x(t)-x)^2 + (y(t)-y)^2})) \quad (1)$$

where ρ is the radius of the obstacle with the centre at (x, y) and α is an empirically defined parameter that is responsible for pushing a path outside of an obstacle. Figure 1 demonstrates the examples of two different selections of α parameter ($\alpha = 0.5$ in the left sub-figure and $\alpha = 0.2$ in the right) for the environment with a single obstacle that is formed by three intersecting circles, shown in Figure 4. Similarly, Figure 2 demonstrates the examples of $\alpha = 0.5$ (in the left sub-figure) and $\alpha = 0.2$ (in the right sub-figure) for the environment with one circular obstacle in the centre and four symmetrical complicated concave obstacles (that are formed by four intersecting circles each), which correspond to the map in Figure 5. In the later example, potential function has clear peaks at the circle intersections.

Topology $T(q)$ is a function that takes into an account all N obstacles of the environment and their influence on the robot along the whole path, which is defined as a parametric function within [0,1]:

$$T(q) = \sum_{j=0}^{N-1} \int_{t=0}^{1} U^{j}{}_{rep}(q) \cdot \delta l(t) \cdot dt \quad (2)$$

where $\delta l(t)$ is simply a length of a segment:

$$\delta l(t) = \sqrt{(x'(t))^2 + (y'(t))^2} \quad (3)$$

A function for smoothness property of the path is referred as *Roughness* $R(q)$ and is also integrated along the path:

$$R(q) = \sqrt{\int_{t=0}^{1} (x''(t))^2 + (y''(t))^2 dt} \quad (4)$$

A function that accounts for the path length $L(q)$ simply sums up the lengths of all path segments:

$$L(q) = \int_{t=0}^{1} \delta l(t) \cdot dt \quad (5)$$

Then, the final path cost function accumulates all the three above components:

$$F(q) = \gamma_1 T(q) + \gamma_2 R(q) + \gamma_3 L(q), \quad (6)$$

where $\gamma_{i=1..3}$ are the weight factors that set an influence of the corresponding component on a total cost of the path. In particular obstacle penalty influence component is empirically defined as $\gamma_1 = \frac{\beta}{2}$, where β ranges over a predefined array, which correlates with array of α parameters from eq.1 (Magid, 2006).

2.2 The Algorithm

The original algorithm of spline-based path planning works iteratively, beginning with start point S and target point T, and utilizes the environment obstacles as its input data. An initial path is suggested as a straight line between points S and T, which serves as a first spline-based path and its spline is defined with three points: S, T and a equidistant point that lies on the straight line between them. Equation 6 sets a current path cost, which is further optimized with Nelder-Mead Simplex Method (Lagarias et al., 1998) in order to minimize the path cost. A resulting *better* path serves as an initial guess for the next iteration.

The optimization procedure operates only with those points of the path, which define its spline, while path evaluation accounts for all points of the path. The path-defining spline is rebuilt at each iteration using information from a previous stage, increasing the number of spline's points by one and adjusting parameters of the target cost function. Once the path is free of obstacles, a few more iterations are conducted in order to improve the resulting path locally. The algorithm terminates if iteration count exceeds a user-defined limit or if a new iteration does not succeed to improve a previous one, while increasing the spline complexity. Figure 3 demonstrates an example of the algorithm successful execution within a simple convex obstacles environment that resembles a plaza with ideal geometrical placement of equal columns or flowerbeds (a view from the above): the initial path is an optimized with regard to eq.6 spline with a single via point between S and T (Figure 3a); after four iterations the spline has four via points but still collides with the obstacles (Figure 3b); after seven iterations the 7-via-points-spline could be already applied for navigation (Figure 3c), but two more iterations succeed to improve path's length and smoothness properties (Figure 3d, 9th iteration); further increase of via points number does not provide any improvement of the path. It took 9 minutes to obtain the final path after 9 iterations of the algorithm.

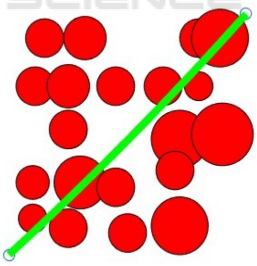
(a)

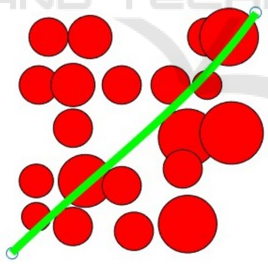
(b)

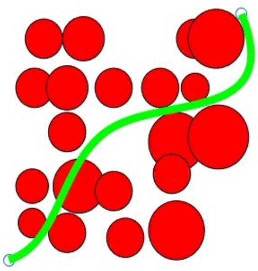
(c)

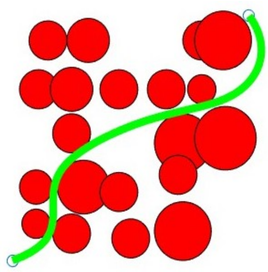
(d)

Figure 3: Simple convex obstacles: (a) the initial state, (b) 4 iterations, (c) 7 iterations, (d) the final path after 9 iterations.

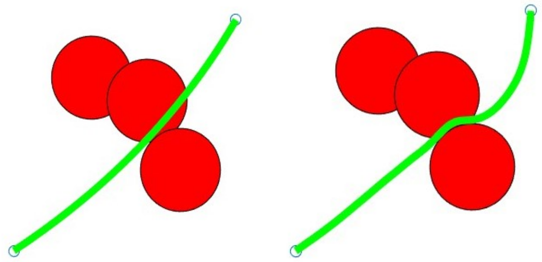

Figure 4: Simple concave obstacle: the first iteration path (left) and the final path after 12 iterations (right).

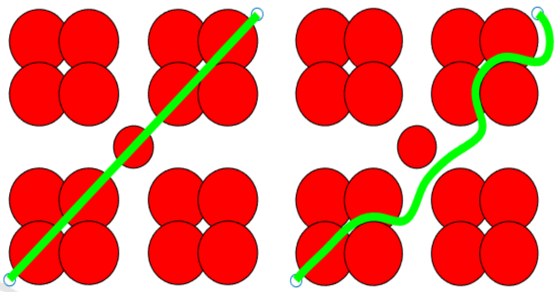

Figure 5: Two complicated concave obstacles: the first iteration path (left) and the final path after 17 iterations (right).

2.3 Drawbacks of the Approach

The original spline-based method succeeds to obtain a collision free smooth path for any complexity of the environment if each obstacle is approximated with a single circle under the condition of non-intersecting obstacles and some minimal distance between the obstacles, which would provide a safety gap for the moving along a path mobile robot. In this case, since the potential function diminishes rapidly as we move away from the obstacle boundary, we could neglect the probability of getting stuck in a local minima. However, when the obstacles are to be approximated with a number of intersecting circles, the intersections introduce potential field local maxima. Moreover, if in such settings an initial spline passes through intersection of several obstacles, the cost function F(q) concentrates on pushing the spline out of intersection area that forms a local maximum; upon successful pushing out, a further solution often gets stuck in a local minima and a next iteration spline can not "jump over" some obstacle components due to a local nature of the optimization process. Figure 4 presents a simple case of an obstacle that is formed by three intersecting circles and the corresponding potential field is presented in Figure 1; after 12 iterations the algorithm stops as no further improvements are possible - while a spline succeeds to optimize the path locally so that it avoids a local maximum, it is still stuck at a local minimum and the resulting path could not be used for navigation due to obstacle collision. Figure 5 demonstrates an example with five complicated concave obstacles and a narrow pass in between. Due to multiple intersecting circles, which generate their own local repulsive potentials, the corresponding global field conceals the pass (Figure 2) and permits only a local optimization of the path. The local optimization successfully avoids local maxima, but even after 37 iterations that continued for 44 minutes, the final path is still occluded with obstacles and thus useless for navigation.

3 INTEGRATING ADDITIONAL OPTIMIZATION CRITERIA

The original spline-based algorithm uses just three criteria within cost function (eq. 6): topology, roughness and length of path. In this section we introduce two new additional criteria - start and target point visibility time - and explore their influence on the resulting path. Point visibility time refers to the path length where the robot keeps the start point (or target point respectively) within its direct line of sight without any obstacle occlusions.

These two criteria are important if a robot needs to maximize the time of a direct visual or radio contact with a monitoring device or a router, which supports path planning, localization or any other functionality of the robot. The criterion should consider the ratio of visible and invisible from the start (or target) points segments of a path. Thus, we need to maximize the time when the robot is visible from the start point while following the selected path before it disappears behind some obstacle for the first time. In other words, we minimize the time (which is actually measured as a length of the path assuming a constant speed of the robot - in our future work we also extend this to the cases of varying speed along the path) after the robot becomes occluded for the first time, which we refer as invisibility of the start point S:

$$I_S = 1 - \lim_{\delta t, \delta l(t) \to 0} \frac{\sum_{t=0}^{u} dist(A(t), A(t+\delta t))}{\int_{t=0}^{1} \delta l(t) \cdot dt} \tag{7}$$

such that

$$\forall t \in [0, u+\delta t] : [A(t), S] \cap (\cup_{j=1}^{N} Obs_j) = \emptyset \tag{8}$$

where the numerator of the fraction in Eq. 7 reflects the path length of a visible from the start position S segment and the denominator of the fraction reflects path length from Eq. 5. $A(t)$ is a position of the robot at timestamp t, and short segments of the path that were travelled between timestamp t and $t+\delta t$, which are denoted by $dist(A(t), A(t+\delta t)$, are accumulated. Eq. 8 describes the visibility property, which means that a straight segment $[A(t), S]$ does not intersect any obstacle Obs_j where $j = 1..N$ and N is a number of obstacles in the environment. Thus, the last visible point from the start point while the robot follows the selected path before disappearing behind an obstacle for the first time is described with $A(u+\delta t)$. Similarly, we describe the criterion that shows the ratio of visible and invisible from the target point segments of a path, which we refer as invisibility of the target point T:

$$I_T = 1 - \lim_{\delta t, \delta l(t) \to 0} \frac{\sum_{t=w}^{1-\delta t} dist(A(t), A(t+\delta t))}{\int_{t=0}^{1} \delta l(t) \cdot dt} \tag{9}$$

such that

$$\forall t \in [w, 1] : [A(t), T] \cap (\cup_{j=1}^{N} Obs_j) = \emptyset \tag{10}$$

Eq. 9 and 10 describe the first point $A(w)$ of a path segment $[A(w), A(1) = T]$ that marks the beginning of the last segment of the path which is featured by a guaranteed constant visual contact between the robot and the target position T while the robot follows the selected path.

The cost function that combines all five criteria is defined as follows:

$$F(q) = \gamma_1 T(q) + \gamma_2 R(q) + \gamma_3 L(q) + \gamma_4 I_S + \gamma_5 I_T, \tag{11}$$

where γ_4 and γ_5 are the weight factors that set the line-of-sight criteria influence on a total cost of the path for start S and target T points respectively. Figure 6 demonstrates the two criteria influence on the path in the vicinity of start and target points: while with γ_4=10 and γ_5=10 these criteria do not contribute any significant influence (left sub-figure), with γ_4=20 and γ_5=20 the path changes are clearly visible, especially as the robot approaches the target position (right sub-figure); other parameters are defined as γ_1=1, γ_2=1, and γ_3=0.5 for both cases (both sub-figures).

As the path optimization with regard to Eq. 11 is performed only locally, the influence of the two additional parameters is also local. As a part of our future work we plan to apply the optimization at a global scale, which will allow the path to vary different homotopy sets in order to satisfy and emphasize a particular user-defined criterion influence.

4 VORONOI DIAGRAM BASED SOLUTION

We recognize that the local nature of the optimization procedure creates a strong dependence of algorithm success or failure on initial spline. In order to

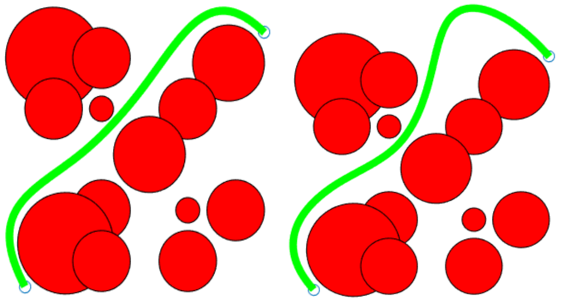

Figure 6: Start and target points visibility time influence on the path quality: γ_4=10, γ_5=10 (left) and γ_4=20, γ_5=20 (right).

provide a good initial spline that could be further improved locally with regard to user selection of the cost weights, we apply Voronoi Diagram approach (Toth et al., 2004). This helps to avoid the spline seizing at local minima.

Assuming the above definition of environment obstacles and potential field, prior to Voronoi graph construction, the two following steps are performed in order to prepare the environment:

1. Register obstacles by grouping intersecting circles together in order to form a single obstacle. Initially, every circle is marked as idle and has its own index $i = 1..M$, where M is a finite number of circles within the environment. We start from an arbitrarily circle, assign it to obstacle O_1 and mark as an activated one. Next, we iteratively grow O_1 by searching for all idle circles that intersect with O_1, assign them to obstacle O_1 and mark as activated as well. The iterative growth of O_1 continues until no more idle circles that intersect O_1 are left in the environment. When the iterative growth of O_1 is completed but there are still idle obstacles available, we select another arbitrarily idle circle, assign it to obstacle O_2 and repeat the growth procedure. Obstacles registration is completed when all circles of the environment become activated. For example, there are five obstacles that are formed by groups of circles in Figure 7 and twelve obstacles in Figure 8. While performing the registration, each pair of intersecting circles i and j provides their intersection point ω_{ij} in a case there is a single joint point (i.e., boundary touch) and a pair of points ω_{ij}, ω_{ji} in a case of joint two points (i.e., boundary intersection).

2. Find outer and inner boundaries of each obstacle of set $Obst = \{O_1, O_2, ..., O_k\}$, where k is a number of compound obstacle within the environment. Starting from an arbitrary circle within O_1 obstacle, boundaries of all circles that belong to O_1 are split into short segments of length σ, merged via intersection points ω_{ij} (or ω_{ji}) and labelled. Parameter σ is predefined in advance and correlates with a radius of a smallest circle of the environment in order to further match a shortest polygonal edge of contours. Thus, during the procedure, two segments receive the same label if there exists a continuous path between them, which is built of boundary segments. This procedure is repeated for each obstacle and upon its completion we receive a set of obstacles' boundaries. If the size of the latter set exceeds the size of $Obst$, it points out a presence of inner boundaries that were formed by internal contours. To get rid of such contours, for each particular obstacle O_i we encapsulated every contour of O_i into a convex hull, verify which of the resulting contours forms outer boundary of O_i and remove the rest. For example, this procedure has successfully removed four tiny diamond-shape internal contours inside complicated obstacles of environment in Figure 7. Finally, we obtain several non-convex polygons, one for each obstacle within $Obst$, and tightly encapsulate them into a square map.

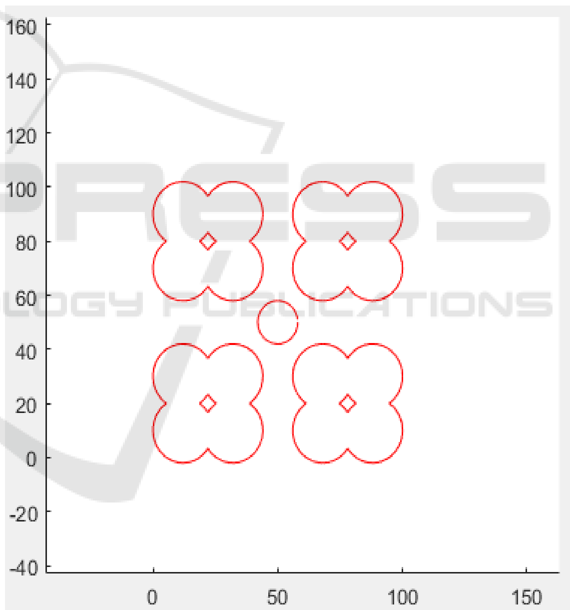

Figure 7: External contours of group of obstacles.

Next, Voronoi graph is constructed as follows, based on a classical brushfire approach (Choset, 2005):

1. Parse free space with rays that originate from obstacles' edges and square map boundary. Figure 8 (the bottom image) demonstrates an example of Voronoi graph construction for the environment in the top image of the figure. Thick blue lines depict borders of obstacles of $Obst$ set and thin blue lines are emerging outwards and inwards rays.

2. Calculate rays intersection points and connect them with segments for neighbouring ray. These

segments are equidistant to nearest obstacles, and all together form Voronoi graph, which is depicted with a thin red line in Figure 8 (the bottom image)

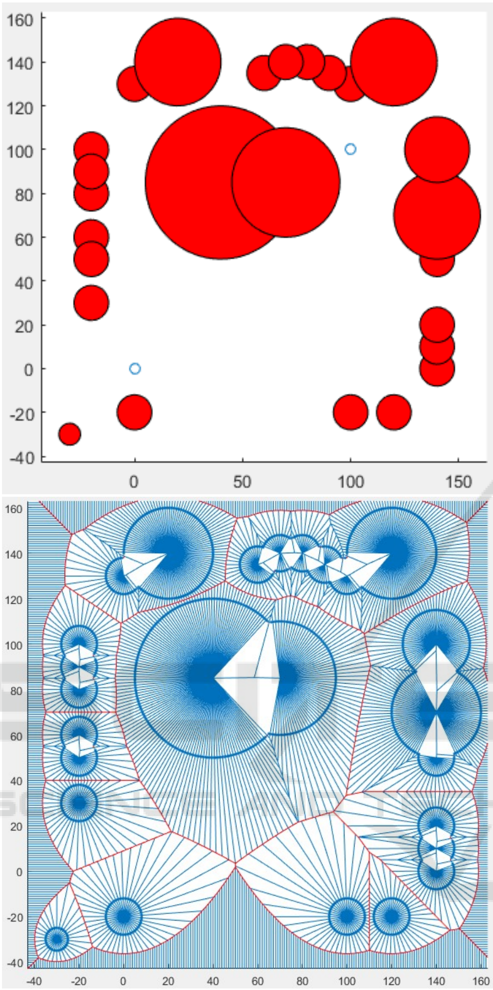

Figure 8: Environment with obstacles (top) and Voronoi graph building procedure (bottom).

Upon obtaining Voronoi graph VG, we select nearest to start position S and target position T points (S' and T' respectively) within VG so that segments $[S,S']$ and $[T,T']$ lie in the free space of the environment. Next, shortest paths between S' and T' are found within VG applying Dijkstra algorithm (Dijkstra, 1959); they are depicted with thick red lines in Figure 9). Any path (S,T) on Voronoi graph VG is guaranteed to be collision free and maximally safe with regard to distance from obstacle boundaries, and thus could provide a good initial spline for the original spline-based method (Magid et al., 2006).

If we use points S, T and Voronoi graph VG nodes (thick red points on Figure 9), which are a part of some selected path (S,T), in a role of via points for

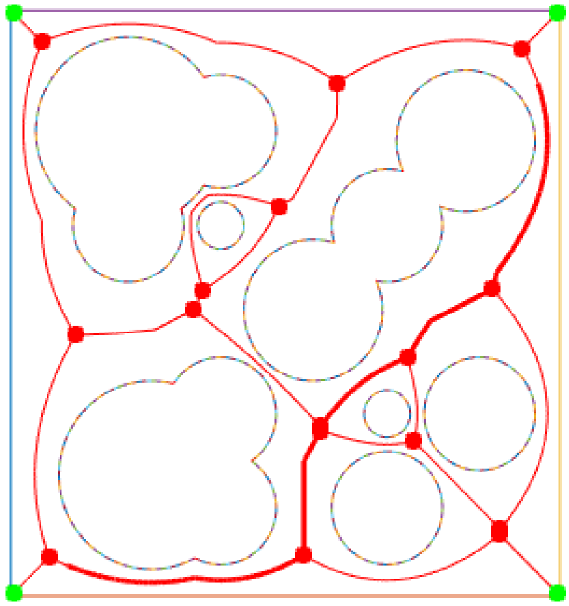

Figure 9: The obtained Voronoi graph and a path within the graph.

initial spline, such sparse selection may fail to guarantee a good start of the spline-based method. On the opposite, selecting every point of some selected path (S,T) provides us with a dense and excess amount of via points. Our trade-off solution that uses a small set of special points of VG (that belong to the path) utilizes only via points that would properly characterize path's features yet avoid redundant complexity of a spline. At a first step, S is selected as a active point and a farthest visible from S point of the path, VP_1, is calculated. S is added to $\{L\}$, while VP_1 receives a status of a next active point and again a farthest visible from VP_1 point of the path, VP_2, is calculated. VP_1 is added to $\{L\}$, VP_2 becomes a next active point and the process continues until target point T becomes visible. Here, point VP_{i+1} is visible from point VP_i if they could be connected with a straight segment that does not collide with any obstacle of the environment. After the process finishes, the points of $\{L\}$ are utilized as via points for initial spline of the spline-based method (Magid et al., 2006).

5 SIMULATIONS

In order to verify our approach the new smart spline-based algorithm was implemented in Matlab environment and an exhaustive set of simulations was performed. Particular attention was paid to the cases where the original algorithm failed (Magid et al., 2006). The cost function of Eq. 11 was applied with

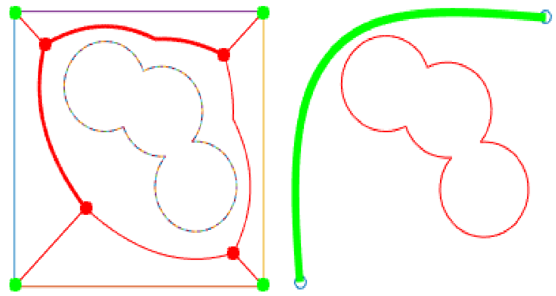

Figure 10: Path planning results: path on Voronoi graph (left) and the corresponding spline-based optimal path (right).

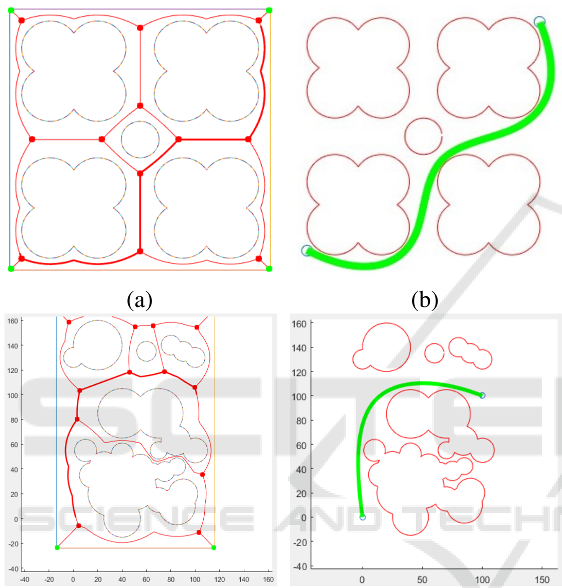

(a) (b) (c) (d)

Figure 11: Path planning results: paths within Voronoi graph (a,c) and the corresponding spline-based optimal paths (b,d).

the following empirical parameter selection: γ_1=1, γ_2=1, γ_3=0.5, γ_4=5, and γ_5=5. The algorithm succeeded to provide collision-free paths in all cases, which was a natural consequence of applying initial Voronoi-based path as an input of our iterative algorithm at the first stage of the procedure.

Figure 11 demonstrates two environments, where the original spline-based algorithm had failed (e.g., the example in sub-figure (b) corresponds to Figure 5). Voronoi graph provides us with a safe path without obstacle collision or may barely touching the obstacle boundaries in a case of very narrow passages between distinct obstacles (of configuration space). Therefore, this good initial path ensures that the modified spline-based algorithm would calculate a final path within a significantly smaller number of iterations. Our preliminary concern about the time complexity of Voronoi graph construction turned out to be obsolete as the simulations empirically demonstrated that Voronoi graph calculations take acceptably small amount of time (at least for our reasonably simple cases, while more simulations in complicated large-size environments are scheduled as a part of the future work).

For example, for the environment of Figure 11(a) the Voronoi-based initial path calculation took only 2 seconds, while for Figure 11(c) - 6 seconds. The total running time of the new algorithm decreased in three times in average with regard to the original algorithm. This way, the final path of Figure 11(b) was calculated in just 2 iterations within 2.5 minutes in Matlab, while the original spline-based algorithm had spent 17 iterations and 44 minutes to conclude on its failure to provide an acceptable path from start to target point. Similarly, the original algorithm required 9 iterations and 15 minutes to provide a good path within Figure 3 environment, while the new algorithm required 5 iterations and 4 minutes. In another case of Figure 4 the original algorithm failed to find a path, while a Voronoi-based algorithm successfully completed the task within 3 iteration and 2 minutes (Figure 10).

6 DISCUSSION AND FUTURE WORK

The computation time in minutes per iteration of our currently implemented spline-based algorithm in its Matlab prototype is an obstacle for dynamical on-line planning with changing or dynamic environments in practical applications. However, we emphasize that a full-scale Voronoi graph construction and path planning are performed off-line before a search and rescue mission starts in order to select an initial path of the vehicle. Then, as the vehicle discovers new or dynamical obstacles on its way, the graph could be rebuilt only locally (e.g., using techniques similar to (Kalra et al., 2009) or creating a local virtual generalized Voronoi graph (Choset et al., 2000)) and local replanning is performed. Local replanning, as well as implementation speed up and optimization, are parts of our ongoing and future work. We strongly believe that C++ implementation will significantly increase all computations.

The selection of $gamma_n$ (n=1, , 5) coefficients in equation (11) is very important for a successful path planning in practical applications. Currently, the selection is performed empirically, which in our opinion is a rather weak point of the algorithm. As one of the possible further extensions of this work, a separate project for theoretical or comparative approach with exhaustive simulations and further analysis of the obtained data would be of a great value for proper selection of these parameters.

Figure 12: Unior robot, courtesy of Avrora robotics company, Russia.

Figure 13: Servosila Engineer mobile robot, courtesy of Servosila company, Russia.

As a part of our future work we plan to introduce some new parameters of cost function, including varying speed of the robot along the path. The algorithm will be tested in large-size environments in order to verify the acceptability of the Voronoi-graph construction time for more complicated cases. We would like to apply optimization procedure at a global scale, which will allow the path to vary different homotopy sets in order to satisfy and emphasize a particular user-defined criterion influence. Moreover, we consider extending the algorithm for 3D environment and adding new parameters of cost function that are associated with 3D surfaces. The algorithm will be bundled into a ROS package with C++ implementation and further verified with real navigation of a heterogeneous robotic team operating in an urban search and rescue scenario. Real experimentation in real world, both static and dynamic, are optimistically scheduled for 2018 and will be executed utilizing Unior car-type mobile robots 12 and a group of DJI Phantom quadcopters. Additional testing will be performed with our crawler "Servosila Engineer" mobile robot 13, in ROS-Gazebo simulation (Sokolov et al., 2016), as well as with a real hardware in order evaluate the applicability of the algorithm for crawler-type robots. In addition, it will be interesting to compare our solution with the adaptive elliptic trajectories for smooth and safe mobile robot navigation approach (Adouane et al., 2011) and trying another representation of complex shaped obstacles in harmonic potential fields (Daily and Bevly, 2008).

7 CONCLUSIONS

A typical difficulty of path planning with potential function methods is getting stuck in local minima of a navigation function. In this paper we have presented a combined method for calculating a smooth and safe path for mobile robot in static planar environment. The introduced modifications of our original spline-based path planning algorithm for a mobile robot navigation helped avoiding local minima problem and added more flexibility for path optimization. We sophisticated the cost function by introducing additional criteria that maximized the time of keeping the robot within direct line of sight from start and target points while the robot follows the path. We also integrated a Voronoi graph approach into the algorithm in order to produce a good starting path for iterative spline-based optimization. The new smart spline-based method algorithm was implemented in Matlab environment and its results were explicitly compared with our original algorithm. The new approach requires less optimization iterations that the original algorithm due to a smart selection of an initial spline. While the original algorithm fails to find an existing path in complicated environments with multiple concave obstacles, its smart version was successful in all simulated tests because of the Voronoi graph approach nature.

ACKNOWLEDGEMENTS

This work was partially supported by the Russian Foundation for Basic Research (RFBR) and Ministry of Science Technology & Space State of Israel (joint project ID 15-57-06010). Part of the work was performed according to the Russian Government Program of Competitive Growth of Kazan Federal University.

REFERENCES

Adouane, L., Benzerrouk, A., and Martinet, P. (2011). Mobile robot navigation in cluttered environment using reactive elliptic trajectories. *IFAC Proceedings Volumes*, 44(1):13801–13806.

Andrews, J. R. and Hogan, N. (1983). Impedance control as a framework for implementing obstacle avoidance in a manipulator. Master's thesis, M. I. T., Dept. of Mechanical Engineering.

Buyval, A., Afanasyev, I., and Magid, E. (2016). Comparative analysis of ros-based monocular slam methods for indoor navigation. *9th International Conference on Machine Vision (ICMV), Nice, France*.

Choset, H. and Burdick, J. (1995). Sensor based planning. i. the generalized voronoi graph. In *Robotics and Automation, 1995. Proceedings., 1995 IEEE International Conference on*, volume 2, pages 1649–1655. IEEE.

Choset, H., Walker, S., Eiamsa-Ard, K., and Burdick, J. (2000). Sensor-based exploration: Incremental construction of the hierarchical generalized voronoi graph. *The International Journal of Robotics Research*, 19(2):126–148.

Choset, H. M. (2005). *Principles of robot motion: theory, algorithms, and implementation*. MIT press.

Daily, R. and Bevly, D. M. (2008). Harmonic potential field path planning for high speed vehicles. In *American Control Conference, 2008*, pages 4609–4614. IEEE.

Dijkstra, E. W. (1959). A note on two problems in connexion with graphs. *Numerische mathematik*, 1(1):269–271.

Elbanhawi, M., Simic, M., and Jazar, R. N. (2015). Continuous path smoothing for car-like robots using b-spline curves. *Journal of Intelligent & Robotic Systems*, 80(1):23–56.

Fleury, S., Soueres, P., Laumond, J.-P., and Chatila, R. (1995). Primitives for smoothing mobile robot trajectories. *IEEE transactions on robotics and automation*, 11(3):441–448.

Indelman, V., Carlone, L., and Dellaert, F. (2015). Planning in the continuous domain: A generalized belief space approach for autonomous navigation in unknown environments. *The International Journal of Robotics Research*, 34(7):849–882.

Kalra, N., Ferguson, D., and Stentz, A. (2009). Incremental reconstruction of generalized voronoi diagrams on grids. *Robotics and Autonomous Systems*, 57(2):123–128.

Khatib, O. and Siciliano, B. (2016). *Springer handbook of robotics*. Springer.

Lagarias, J. C., Reeds, J. A., Wright, M. H., and Wright, P. E. (1998). Convergence properties of the nelder–mead simplex method in low dimensions. *SIAM Journal on optimization*, 9(1):112–147.

Latombe, J.-C. (2012). *Robot motion planning*, volume 124. Springer Science & Business Media.

Magid, E. (2006). Sensor-based robot navigation. Master's thesis, Technion - Israel Institute of Technology.

Magid, E., Keren, D., Rivlin, E., and Yavneh, I. (2006). Spline-based robot navigation. In *Intelligent Robots and Systems, 2006 IEEE/RSJ International Conference on*, pages 2296–2301. IEEE.

Magid, E., Tsubouchi, T., Koyanagi, E., and Yoshida, T. (2011). Building a search tree for a pilot system of a rescue search robot in a discretized random step environment. *Journal of Robotics and Mechatronics*, 23(4):567.

Panov, A. I. and Yakovlev, K. (2017). *Behavior and Path Planning for the Coalition of Cognitive Robots in Smart Relocation Tasks*, pages 3–20. Springer International Publishing, Cham.

Pipe, A., Dailami, F., and Melhuish, C. (2014). Crucial challenges and groundbreaking opportunities for advanced hri. In *System Integration (SII), 2014 IEEE/SICE International Symposium on*, pages 12–15. IEEE.

Ronzhin, A., Vatamaniuk, I., and Pavluk, N. (2016). Automatic control of robotic swarm during convex shape generation. In *Electrical and Power Engineering, 2016 International Conference and Exposition on*, pages 675–680. IEEE.

Rosenfeld, A., Agmon, N., Maksimov, O., Azaria, A., and Kraus, S. (2015). Intelligent agent supporting human-multi-robot team collaboration. In *Proceedings of the 24th International Conference on Artificial Intelligence*, pages 1902–1908. AAAI Press.

Seraji, H. (1999). Traversability index: A new concept for planetary rovers. In *Robotics and Automation, 1999. Proceedings. 1999 IEEE International Conference on*, volume 3, pages 2006–2013. IEEE.

Sokolov, M., Lavrenov, R., Gabdullin, A., Afanasyev, I., and Magid, E. (2016). 3d modelling and simulation of a crawler robot in ros/gazebo. In *Proceedings of the 4th International Conference on Control, Mechatronics and Automation*, pages 61–65. ACM.

Tang, L., Dian, S., Gu, G., Zhou, K., Wang, S., and Feng, X. (2010). A novel potential field method for obstacle avoidance and path planning of mobile robot. In *Computer Science and Information Technology (ICCSIT), 2010 3rd IEEE International Conference on*, volume 9, pages 633–637. IEEE.

Toth, C. D., O'Rourke, J., and Goodman, J. E. (2004). *Handbook of discrete and computational geometry*. CRC press.